The Electronic Properties of Au and Pt Metal Contacts on Quasi-One-Dimensional Layered TiS_3(001)

Simeon J. Gilbert[1], Alexey Lipatov[2], Andrew J. Yost[1], Alexander Sinitskii[2,3], and Peter A. Dowben[1*]

[1]Department of Physics and Astronomy, University of Nebraska-Lincoln, Lincoln, NE 68588-0299, U.S.A.

[2]Department of Chemistry, University of Nebraska-Lincoln, Lincoln, NE 68588-0304, U.S.A.

[3]Nebraska Center for Materials and Nanoscience, University of Nebraska-Lincoln, Lincoln, NE 68588-0298, U.S.A.

*Corresponding Author: pdowben@unl.edu

Abstract

The interfaces of the layered trichalcogenide TiS_3(001), with the metals Au and Pt, were examined using X-ray photoemission spectroscopy. In spite of the fact that both Au and Pt are large work function metals, no evidence of Schottky barrier formation was found with this n-type semiconductor. Two- and four-terminal field-effect transistor measurements performed on exfoliated few-nm-thick TiS_3 crystals using pure Au contacts indicate that Au forms an Ohmic contact on TiS_3(001), with negligible contact resistance. The absence of appreciable Schottky barrier formation is attributed to strong interactions with sulfur at the metal-semiconductor interface.

Transition metal trichalcogenides (TMTs) have garnered increased attention from researchers in recent years for use in nanoelectronics and optoelectronics.[1–9] The Group IV trichalcogenides, such as TiS_3, are notable for their quasi-one-dimensional (1D) structure,[1] which is comprised of 1D chains of covalently bonded MX_3 trigonal prisms assembled into two-dimensional (2D) sheets by means of weak van der Waals-like bonding (Figure 1a).[10] Because of their quasi-1D structure, TiS_3 crystals typically grow in a form of needle-like crystals (Figure 1b) with their long axes corresponding to the crystallographic *b* direction of 1D chains, as indicated in transmission electron microscopy (TEM) in Figure 1c. Similar to other 2D materials, these TiS_3 whiskers can be mechanically exfoliated into few-layer or even monolayer crystals using an adhesive tape.[10] The TMTs are favored over other 2D materials because the quasi-1D TMTs are uniquely suited to address edge scattering effects. By way of comparison, 2D materials such as graphene and the transition metal dichalcogenides experience significant edge scattering effects in sub-10 nm devices, as is evident in both theory[11–14] and experiment.[15–17] The smallest structural unit of the TMTs, a 1D chain of MX_3 prisms (Figure 1a,c), is atomically smooth and free from dangling bonds or stabilizing functional groups, which significantly reduces the number of edge defects compared to the rough edges of patterned or exfoliated 2D materials. The transport within the 2D plane of these TMTs is also highly anisotropic resulting in preferential charge transport along the chain direction, while minimizing edge scattering.[1,4]

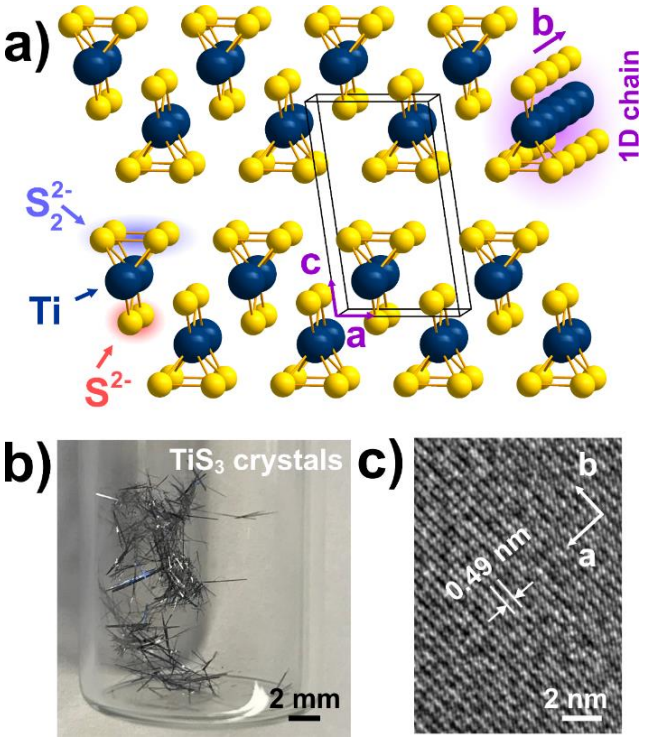

Figure 1. (a) Scheme of the monoclinic TiS_3 crystal structure with a P21/m space group. (b) Optical photograph of TiS_3 crystals. (c) High-resolution TEM image of the 1D chains oriented along the b crystallographic direction in TiS_3 crystal. The image was recorded using a FEI Tecnai Osiris scanning transmission electron microscope at the accelerating voltage of 200 kV.

Among the various transition metal trichalcogenides, TiS_3 shows exceptional promise due to its favorable band gap (~1 eV) and predicted high electron mobility (~10,000 $cm^2V^{-1}s^{-1}$)[18] for a monolayer sheet, which has resulted in research on its potential for field-effect transistors (FETs)[3,4,19] as well as optoelectronics.[2,20–23] The experimentally measured mobility of few-layer TiS_3 FETs has never exceeded 100 $cm^2V^{-1}s^{-1}$, and remains two orders of magnitude below predictions.[3,4,19,23,24] This discrepancy is not surprising as the first graphene field-effect transistors had mobilities of a few hundred $cm^2V^{-1}s^{-1}$, which was improved to over 100,000 $cm^2V^{-1}s^{-1}$ with proper device optimization.[25,26] Recently, phonon scattering has been implicated in the reduction

of electron mobility in TiS_3,[27] but another explanation for low electron mobility is the formation of a Schottky barrier which has inhibited the performance of other 2D materials.[4,28] Previous experiments on TiS_3 have utilized Cr/Au[3,27] or Ti/Au[4,19,23] contacts, with the Ti/Au contacts exhibiting evidence of a Schottky barrier[4] while the Cr/Au contacts seem to create Ohmic contacts.[3,27] In both cases, Au was not the direct contact metal with TiS_3. Higher work function metals, such as Au, are generally expected to form larger Schottky barriers on n-type semiconductors,[29] such as TiS_3.[1] This trend has previously been observed for 2D MoS_2.[28] In this work we studied the interface between TiS_3 and the high work function metals Au and Pt by means of X-ray photoemission spectroscopy (XPS) and electrical transport measurements of TiS_3 FETs.

For this experiment, TiS_3 whiskers were synthesized by the direct reaction of titanium and sulfur as discussed in previous studies.[1,3,21] The TiS_3 surface was prepared for XPS study through an exfoliation method where adhesive tape was attached to TiS_3 while in atmosphere and then removed in ultra-high vacuum (UHV). The XPS was performed with a VG100AX hemispherical analyzer using non-monochromatized Al-Kα X-ray radiation. All XPS was performed at room temperature in an ultra-high vacuum chamber. The metal deposition was performed in UHV through the resistive heating of Au and Pt wires in a tungsten wire basket. The maximum Au and Pt thicknesses were calculated as 14 Å and 17 Å, based on the changes in core level XPS photoelectron peak intensities as discussed in previous studies.[30,31]

For electrical transport measurements, we fabricated a four-terminal TiS_3 field-effect transistor with Au contacts, for which the TiS_3 was mechanically exfoliated and transferred onto a p-type silicon substrate with a 300 nm surface layer of SiO_2. A few layer thick TiS_3 whisker, approximately 12 nm in height and 0.11 μm wide, was selected for device fabrication. Au contacts were fashioned through electron-beam lithography and electron-beam evaporation so that Au was

in direct contact with the TiS_3 nanowhisker. The TiS_3 FET was placed in a Lake Shore TTPX cryogenic probe station with a base pressure of about 2×10^{-6} Torr. The electrical characteristics of the device were recorded at room temperature using an Agilent 4155C semiconductor parameter analyzer.

The X-ray photoemission spectra for the core level S 2p and Ti 2p photoelectron features with increasing Au and Pt coverage are shown in Figure 2. The Ti $2p_{3/2}$ and $2p_{1/2}$ core level features were fit with a single peak using a standard Voigt distribution function with a 70% Gaussian to 30% Lorentzian, weighting; however, the S 2p core level spectra required multiple peaks, for any fitting, due to the distinct S environments in TiS_3. The two S environments (labeled S_2^{2-} and S^{2-}) are illustrated in Figure 3a. Each S ion contributes two photoelectron core level features ($2p_{3/2}$ and $2p_{1/2}$) which are separated by 1.2 eV. Thus the total spectrum contains 4 peaks as seen in Figure 3b. However, the overlap of the S_2^{2-} $2p_{3/2}$ and the S^{2-} $2p_{1/2}$ peaks cause the appearance of a triplet like feature, with peak positions at roughly 161.1 eV, 162.3 eV and 163.5 eV.[1,32,33]

The convention for high work function metals, such as Au (5.1 eV[34] to 5.4 eV[35]) and Pt (5.5 eV[34,36,37] to 5.93 eV[38]), is that such metal contacts form Schottky barriers on n-type semiconductors,[29] such as TiS_3.[1] The Schottky barrier formation occurs as the result of upward band bending at the metal-semiconductor interface, and will be reflected in XPS as a shift in the semiconductor's core level features toward lower binding energies.[29,39] Figure 4 shows the measured Ti 2p and S 2p binding energies as the metal overlayer thickness is increased. In the case of Au on TiS_3, there is no observed binding energy shift for either the S 2p or Ti 2p photoelectron core level features. For Pt adlayers on TiS_3, the Ti 2p binding energies are reduced by ~0.25 eV, but the S 2p binding energies remain unchanged, with increasing Pt coverage. The near constant S 2p core level binding energies, evident in XPS, indicates that the shift to lower binding energies

for the Ti 2p core level features, with increasing Pt coverage on TiS_3, is not related to the formation of a Schottky barrier as will be discussed below. In fact, neither the Au/TiS_3 nor Pt/TiS_3 XPS data is consistent with the formation of a Schottky barrier.

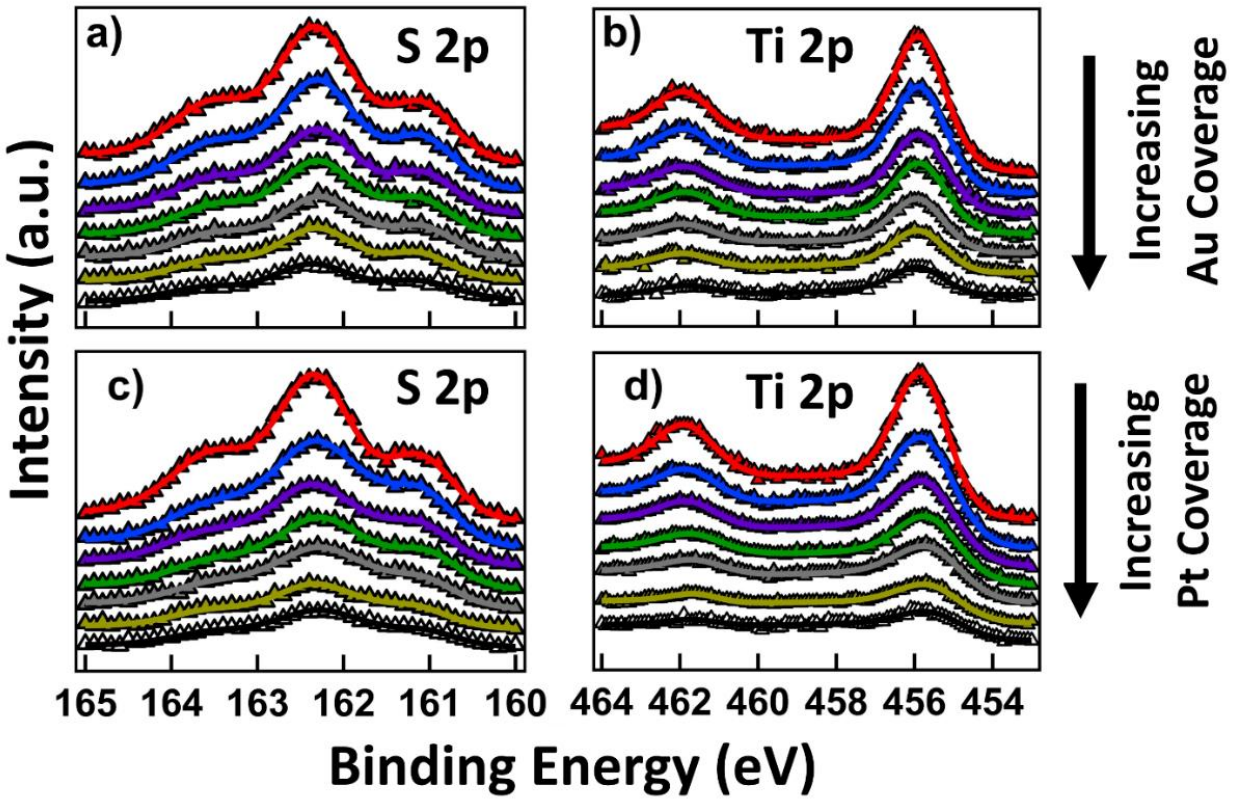

Figure 2. X-ray photoemission spectroscopy of the S 2p and Ti 2p core level features in TiS_3 with increasing Au (a,b) or Pt (c,d) coverage. Triangles represent experimental data and solid lines are the result of profile fitting.

The unexpected absence of a Schottky barrier can be explained through close examination of the S 2p photoelectron core level features. The topmost sulfur curves, red lines, in Figure 2a and 2c correspond to clean TiS_3 and were fit using the same parameters as our previous work,[1] as

shown in Figure 3b. For pure TiS_3, the ratio of the two types of sulfur species, S_2^{2-}:S^{2-}, is ~2:1. As the metal coverage increases, the S_2^{2-}:S^{2-} ratio is expected to increase because the termination layer is comprised of S_2^{2-} ions, and photoemission is surface sensitive. However, as the Au thickness increases the S_2^{2-}:S^{2-} ratio decreases as seen in the inset of Figure 3c. This indicates some form of Au-S interaction with the surface S_2^{2-} ions which reduces the S_2^{2-} XPS signal intensity. This interaction does not appear to be the formation of traditional bonds because there are no additional peaks in the S 2p fitting (Figure 3c) and the Ti 2p core level features appear unaffected by the Au-S interaction (Figure 4a-b). On the other hand, the Pt/TiS_3 system shows indications of appreciable bonding at the metal-semiconductor interface. As the Pt coverage increases, the relative S_2^{2-} intensity once again decreases, but the shoulder-like S 2p core level features are also smoothed appreciably (Figure 3d). As a result, the S 2p XPS data, obtained with increasing Pt coverage on TiS_3, cannot be fit well using only two doublets. For a proper fit of the S 2p features in the Pt/TiS_3 system, a third doublet (red peaks in Figure 3d) was introduced with peak positions at 161.7 eV and 162.9 eV. These peak positions are very similar to the S 2p core level features in TiS_2[1] and are likely the result of a complex Pt-S_2-Ti bonding environment. This is further indicated by the shift to lower binding energy for the Ti 2p core level features (Figure 4a-b) which indicates that the presence of Pt at the interface changes the Ti bonding environment. For both Au and Pt contacts, the metal-S interactions can explain the lack of a Schottky barrier, indicating that in these cases the interface chemistry is a more significant factor than the metal's work function.

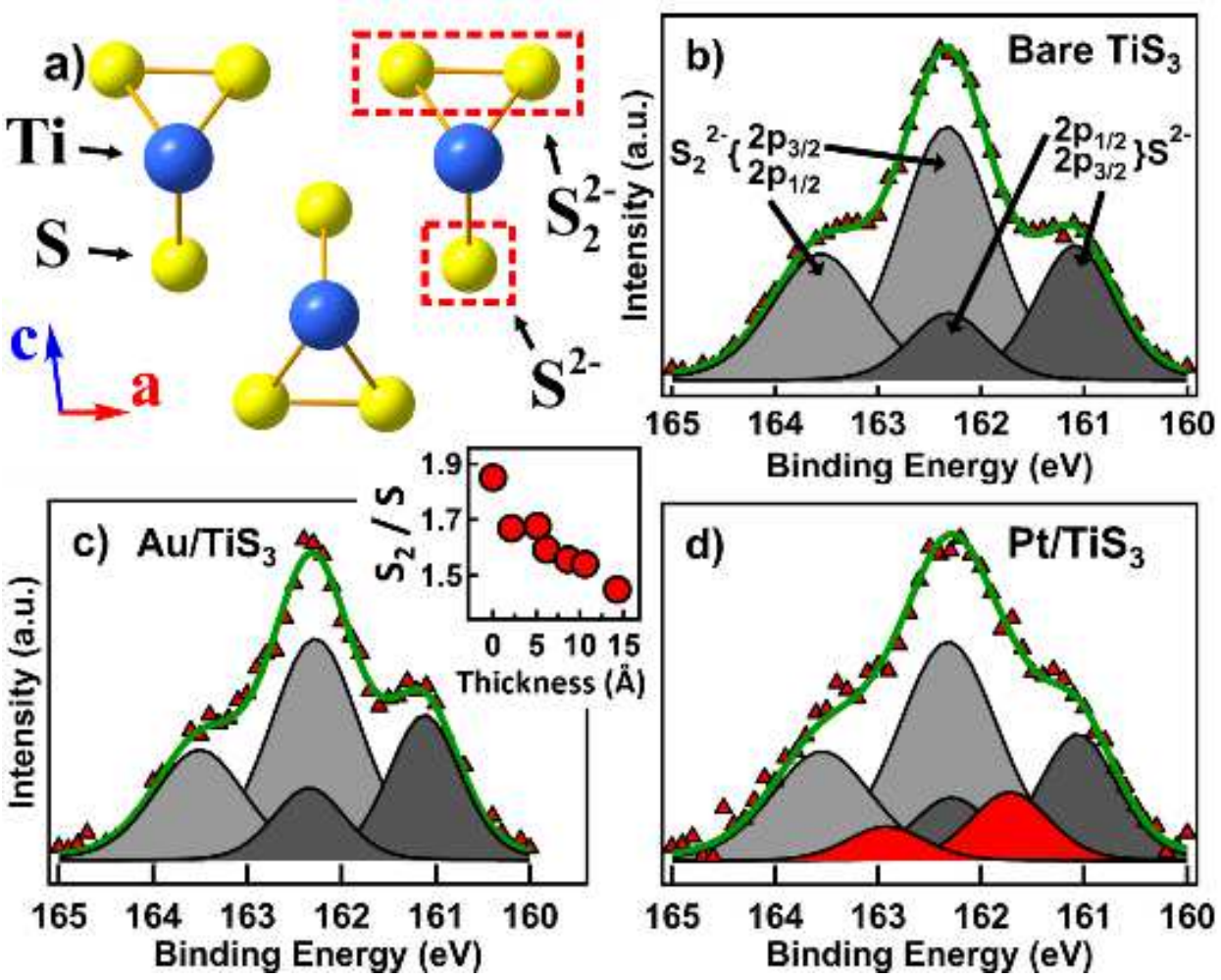

Figure 3. a) The atomic structure of TiS_3 highlighting the different sulfur environments. b) The individual S_2^{2-} (light gray) and S^{2-} (dark gray) peaks used to fit the S 2p XPS spectra for clean TiS_3. c) The XPS fitting for TiS_3 with a 14 Å adlayer of Au. The inset shows the change in the S_2^{2-}/S^{2-} intensity ratio as a function of Au adlayer thickness. d) The XPS fitting for TiS_3 with a 17 Å adlayer of Pt. Red peaks correspond to a Pt-S_2-Ti environment at the interface.

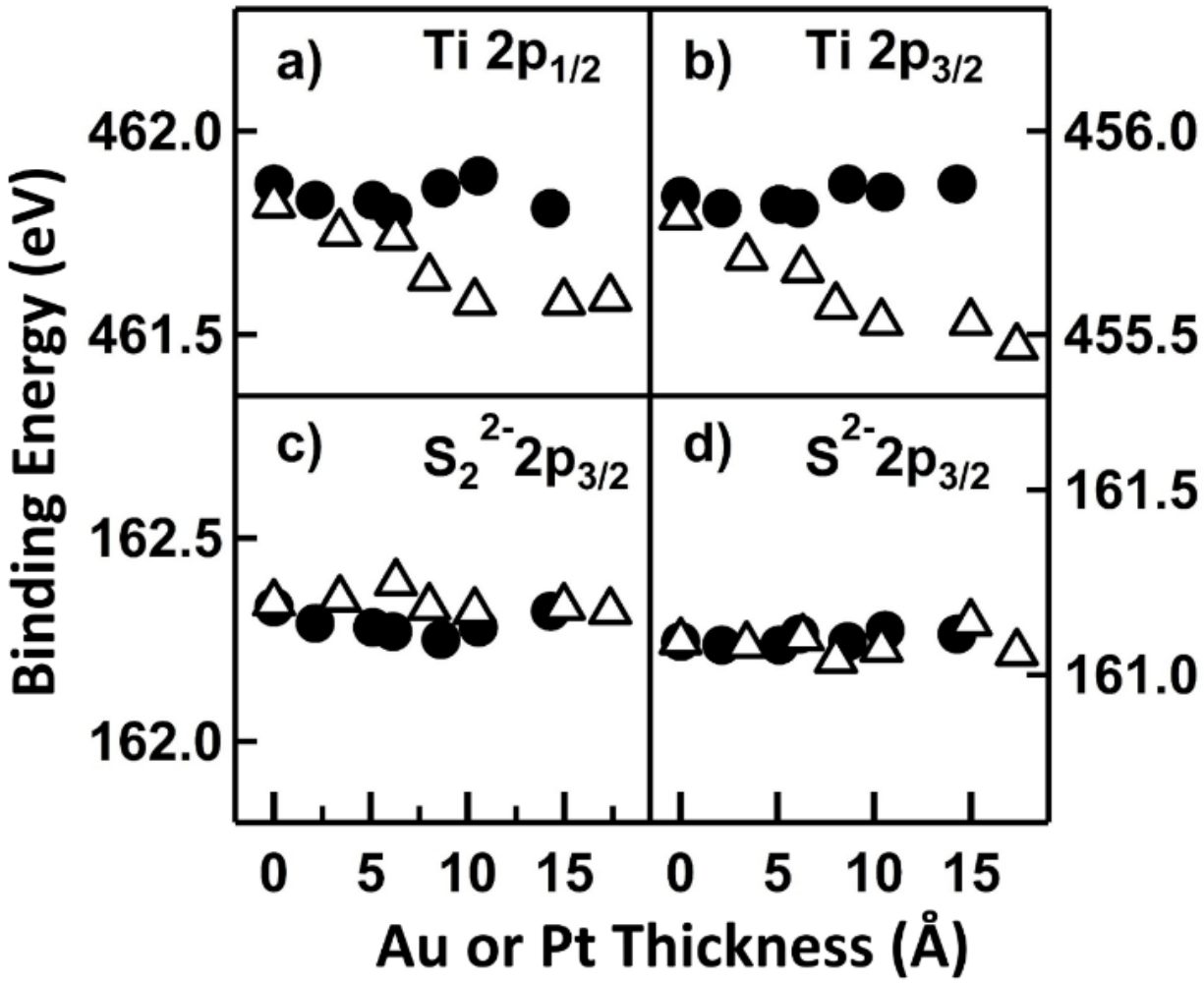

Figure 4. The change in binding energy, as seen in XPS, for the Ti 2p and S 2p photoelectrons in TiS_3 with increasing Au (black circles) or Pt (white triangles) coverage.

To support these claims, a four-terminal TiS_3 field-effect transistor was fabricated using Au contacts. The scanning electron microscopy image in the inset of Figure 5a shows the device, with the source (S), drain (D), as well as V_1 and V_2 voltage probes labelled. In the field-effect measurements the p-doped Si substrate served as a bottom gate (G) electrode. The main panel of Figure 5a presents the results of four-terminal measurements at zero gate bias, showing drain-

source current (I_{DS}) as a function of drain-source voltage (V_{DS}; red curve) and as a function of the voltage drop between the V_1 and V_2 electrodes (V_{12}; blue curve), which was measured while V_{DS} was applied. Both I-V curves are linear, indicating Ohmic behavior rather than the presence of a Schottky barrier. The results are similar to the I-V curves obtained for TiS_3 FETs with Ti/Au and Cr/Au contacts.[2–4,27] The channel resistance measured in the four-terminal configuration was found to be R_{ch} = 1835 kΩ. With a channel length of 6.9 µm and channel width of 0.11 µm, the calculated sheet resistance is about 29 kΩ/□. The estimated contact resistance at zero gate bias calculated from four-terminal measurements was found to be about 1 Ω·cm. This contact resistance is an order of magnitude lower than a MoS_2 FET with Au contacts,[40] which is believed to form a contact tunnel barrier of 1.03 eV.[41]

In Figure 5b we plot transfer curves of the central segment of the TiS_3 device (inset in Figure 5a), which was measured in a two-terminal configuration, when the current through the central segment was measured while applying a potential difference directly between the V_1 and V_2 electrodes, and a four-terminal configuration, when the outer S and D electrodes were used to source current through the TiS_3 crystal, and the inner electrodes were used to measure the V_2-V_1 potential difference. From these graphs, the electron mobility was extracted and found to be 11 $cm^2V^{-1}s^{-1}$ and 12 $cm^2V^{-1}s^{-1}$ in the two- and four-terminal configurations, respectively. The difference in the electron mobility between the different configurations is negligible indicating that the contact resistance present in the two-terminal configuration is not a significant factor in electronic characteristics of the TiS_3 channel. Another TiS_3 device prepared simultaneously with the presented one, but in only the two-terminal configuration, showed an electron mobility of 27 $cm^2V^{-1}s^{-1}$, which is comparable to values obtained for devices with Cr/Au and Ti/Au contacts.[3,4,23] The fact that Ohmic contacts do not vastly improve the electron mobility indicates that the contact

resistance is not always the dominant factor leading to a reduction in the measured electron mobility. Other factors such as the substrate choice, electron-phonon coupling,[27] etc. must be explored in order to explain the discrepancy between the theoretical (~10,000 $cm^2V^{-1}s^{-1}$)[18] and experimental (<100 $cm^2V^{-1}s^{-1}$)[3,4,19,23,27] electron mobility in TiS_3.

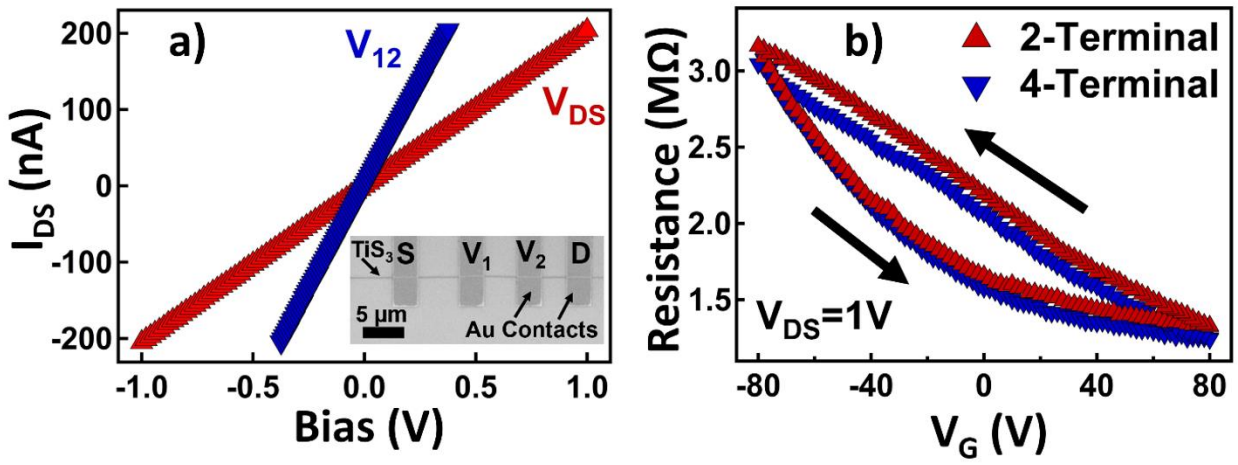

Figure 5. a) The I-V curves obtained from four-terminal measurements of a TiS_3 FET with Au electrodes at zero gate bias. The inset shows the device structure. b) The resistance as a function of gate voltage in both the 2-terminal (red) and 4-terminal (blue) configurations for the same TiS_3 device segment.

In summary, XPS provides clear indications that the contact metals Au and Pt experience strong interface interactions with the sulfur in TiS_3(001). These strong interactions may be why Schottky barrier formation is suppressed for Au or Pt on TiS_3(001), in spite of the high work function of these metals. Additionally, device measurements show negligible contact resistance between Au and TiS_3. However, the electron mobility measured, using Au contacts, was not found to be significantly higher than what was measured in other TiS_3 devices, where Schottky barrier

formation is present. A small contact resistance or Schottky barrier, on the order of a few meV, as reported for Cr/Au contacts on TiS_3,[27] cannot *a priori* be excluded on the basis of the measurements reported here, but any such Schottky barrier would have minimal effects on room temperature device performance.

This research was supported by the National Science Foundation (NSF), through grants NSF-ECCS 1740136, as well as by the nCORE, a wholly owned subsidiary of the Semiconductor Research Corporation (SRC), through the Center on Antiferromagnetic Magneto-electric Memory and Logic task #2760.002. The device fabrication and characterization were performed using instrumentation in the Nebraska Nanoscale Facility, which is supported by the NSF (ECCS-1542182) and the Nebraska Research Initiative.

References

[1] H. Yi, T. Komesu, S. Gilbert, G. Hao, A.J. Yost, A. Lipatov, A. Sinitskii, J. Avila, C. Chen, M.C. Asensio, and P.A. Dowben, Appl. Phys. Lett. **112**, 1 (2018).

[2] J.O. Island, M. Buscema, M. Barawi, J.M. Clamagirand, J.R. Ares, C. Sánchez, I.J. Ferrer, G.A. Steele, H.S.J. van der Zant, and A. Castellanos-Gomez, Adv. Opt. Mater. **2**, 641 (2014).

[3] A. Lipatov, P.M. Wilson, M. Shekhirev, J.D. Teeter, R. Netusil, and A. Sinitskii, Nanoscale **7**, 12291 (2015).

[4] J.O. Island, M. Barawi, R. Biele, A. Almazán, J.M. Clamagirand, J.R. Ares, C. Sánchez, H.S.J. Van Der Zant, J. V. Álvarez, R. D'Agosta, I.J. Ferrer, and A. Castellanos-Gomez, Adv. Mater. **27**, 2595 (2015).

[5] W.-W. Xiong, J.-Q. Chen, X.-C. Wu, and J.-J. Zhu, J. Mater. Chem. C **2**, 7392 (2014).

[6] Y.R. Tao, J.J. Wu, and X.C. Wu, Nanoscale **7**, 14292 (2015).

[7] S. Yang, M. Wu, W. Shen, L. Huang, S. Tongay, K. Wu, B. Wei, Y. Qin, Z. Wang, C. Jiang, and C. Hu, ACS Appl. Mater. Interfaces acsami.8b19050 (2019).

[8] S.G. Zybtsev, V. Ya Pokrovskii, V.F. Nasretdinova, S. V Zaitsev-Zotov, V. V Pavlovskiy, A.B. Odobesco, W. Wu Pai, M. Chu, Y.G. Lin, E. Zupanič, H.J. P van Midden, S. ˇ Sturm, E. Tchernychova, A. Prodan, J.C. Bennett, I.R. Mukhamedshin, O. V Chernysheva, A.P. Menushenkov, V.B. Loginov, B.A. Loginov, A.N. Titov, and M. Abdel-Hafiez, Phys. Rev. B **95**, 35110 (2017).

[9] I.G. Gorlova, S.G. Zybtsev, V.Y. Pokrovskii, N.B. Bolotina, I.A. Verin, and A.N. Titov, Phys.

B Condens. Matter **407**, 1707 (2012).

[10] A. Lipatov, M.J. Loes, H. Lu, J. Dai, P. Patoka, N.S. Vorobeva, D.S. Muratov, G. Ulrich, B. Kästner, A. Hoehl, G. Ulm, X.C. Zeng, E. Rühl, A. Gruverman, P.A. Dowben, and A. Sinitskii, ACS Nano **12**, 12713 (2018).

[11] E.R. Mucciolo and C.H. Lewenkopf, J. Phys. Condens. Matter **22**, 273201 (2010).

[12] J. Wurm, K. Richter, and İ. Adagideli, Phys. Rev. B **84**, 075468 (2011).

[13] V.K. Dugaev and M.I. Katsnelson, Phys. Rev. B **88**, 235432 (2013).

[14] M. Wimmer, İ. Adagideli, S. Berber, D. Tománek, and K. Richter, Phys. Rev. Lett. **100**, 177207 (2008).

[15] Yinxiao Yang and R. Murali, IEEE Electron Device Lett. **31**, 237 (2010).

[16] M.Y. Han, J.C. Brant, and P. Kim, Phys. Rev. Lett. **104**, 056801 (2010).

[17] Y.-J. Shi, J. Lan, E.-J. Ye, W.-Q. Sui, and X. Zhao, Eur. Phys. J. B **87**, 251 (2014).

[18] J. Dai and X.C. Zeng, Angew. Chemie - Int. Ed. **54**, 7572 (2015).

[19] A.J. Molina-Mendoza, J.O. Island, W.S. Paz, J.M. Clamagirand, J.R. Ares, E. Flores, F. Leardini, C. Sánchez, N. Agraït, G. Rubio-Bollinger, H.S.J. van der Zant, I.J. Ferrer, J.J. Palacios, and A. Castellanos-Gomez, Adv. Funct. Mater. **27**, 1605647 (2017).

[20] I.J. Ferrer, M.D. Maciá, V. Carcelén, J.R. Ares, and C. Sánchez, Energy Procedia **22**, 48 (2011).

[21] Q. Cui, A. Lipatov, J.S. Wilt, M.Z. Bellus, X.C. Zeng, J. Wu, A. Sinitskii, and H. Zhao, ACS Appl. Mater. Interfaces **8**, 18334 (2016).

[22] I.J. Ferrer, J.R. Ares, J.M. Clamagirand, M. Barawi, and C. Sánchez, Thin Solid Films **535**, 398 (2013).

[23] J.O. Island, R. Biele, M. Barawi, J.M. Clamagirand, J.R. Ares, C. Sánchez, H.S.J. Van Der Zant, I.J. Ferrer, R. D'Agosta, and A. Castellanos-Gomez, Sci. Rep. **6**, 1 (2016).

[24] E. Finkman and B. Fisher, Solid State Commun. **50**, 25 (1984).

[25] C.R. Dean, A.F. Young, I. Meric, C. Lee, L. Wang, S. Sorgenfrei, K. Watanabe, T. Taniguchi, P. Kim, K.L. Shepard, and J. Hone, Nat. Nanotechnol. **5**, 722 (2010).

[26] L. Wang, I. Meric, P.Y. Huang, Q. Gao, Y. Gao, H. Tran, T. Taniguchi, K. Watanabe, L.M. Campos, D.A. Muller, J. Guo, P. Kim, J. Hone, K.L. Shepard, and C.R. Dean, Science **342**, 614 (2013).

[27] M. Randle, A. Lipatov, A. Kumar, C.-P. Kwan, J. Nathawat, B. Barut, S. Yin, K. He, N. Arabchigavkani, R. Dixit, T. Komesu, J. Avila, M.C. Asensio, P.A. Dowben, A. Sinitskii, U. Singisetti, and J.P. Bird, ACS Nano **13**, 803 (2018).

[28] S. Das, H.-Y. Chen, A.V. Penumatcha, and J. Appenzeller, Nano Lett. **13**, 100 (2013).

[29] Z. Zhang and J.T. Yates, Chem. Rev. **112**, 5520 (2012).

[30] M.P. Seah, Surf. Interface Anal. **44**, 1353 (2012).

[31] J. Walton, M.R. Alexander, N. Fairley, P. Roach, and A.G. Shard, Surf. Interface Anal. **48**, 164 (2016).

[32] M.E. Fleet, S.L. Harmer, X. Liu, and H.W. Nesbitt, Surf. Sci. **584**, 133 (2005).

[33] K. Endo, H. Ihara, K. Watanabe, and S.-I. Gonda, J. Solid State Chem. **44**, 268 (1982).

[34] D.E. Eastman, Phys. Rev. B **2**, 1 (1970).

[35] H.C. Potter and J.M. Blakely, J. Vac. Sci. Technol. **12**, 635 (1975).

[36] D.M. Collins, J.B. Lee, and W.. Spicer, Surf. Sci. **55**, 389 (1976).

[37] R.I. Mints, V.P. Melekhin, and M.B. Partenskii, Sov. Phys. Sol. State **16**, 2330 (1975).

[38] P.E.C. Franken and V. Ponec, Surf. Sci. **53**, 341 (1975).

[39] E. Echeverría, G. Peterson, B. Dong, S. Gilbert, A. Oyelade, M. Nastasi, J.A. Kelber, and P.A. Dowben, Zeitschrift Fur Phys. Chemie **232**, 893 (2018).

[40] S.-L. Li, K. Komatsu, S. Nakaharai, Y.-F. Lin, M. Yamamoto, X. Duan, and K. Tsukagoshi, ACS Nano **8**, 12836 (2014).

[41] I. Popov, G. Seifert, and D. Tománek, Phys. Rev. Lett. **108**, 156802 (2012).

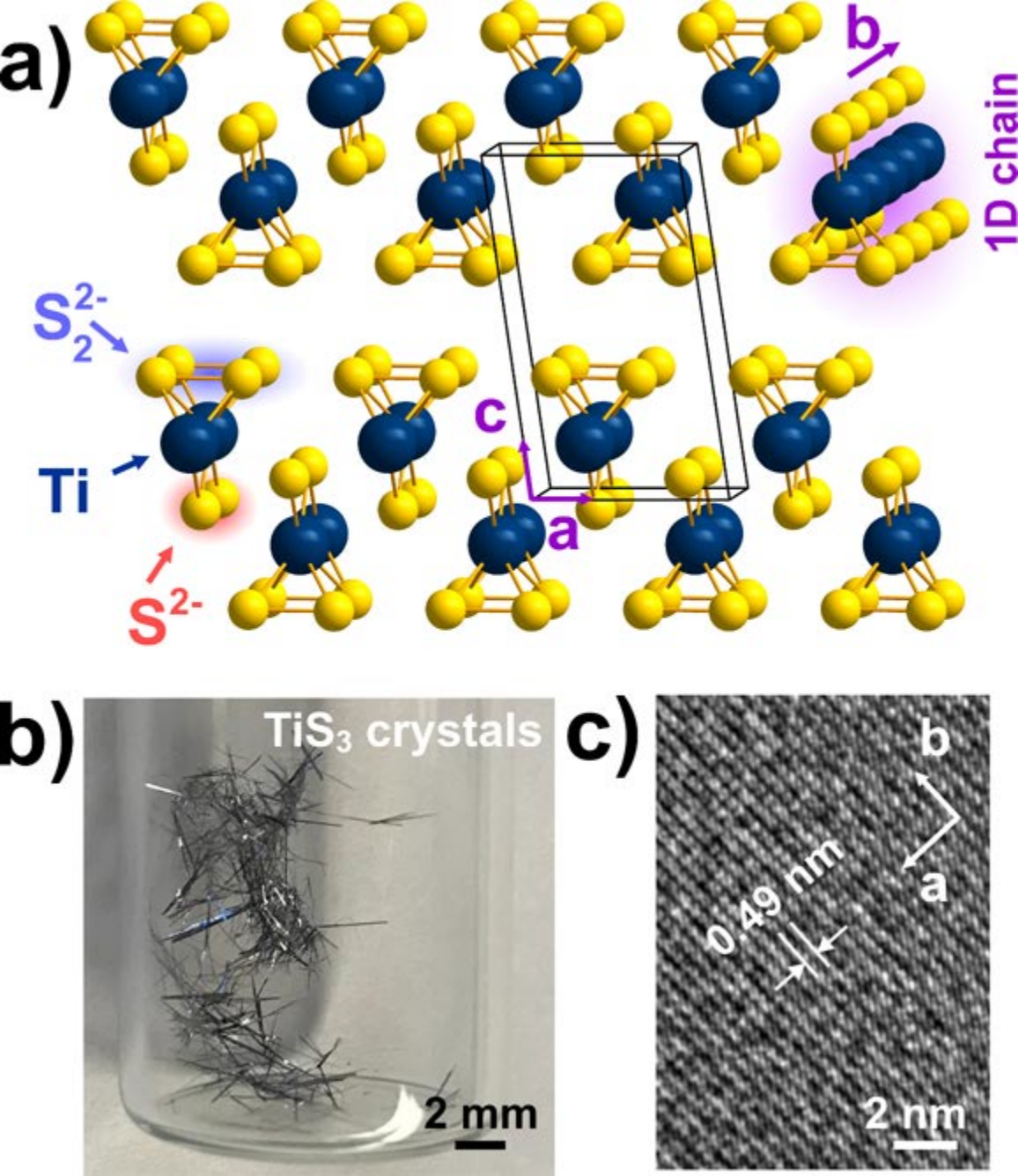
a)
b
1D chain
S_2^{2-}
Ti
S^{2-}
c
a
b)
TiS_3 crystals
2 mm
c)
b
a
0.49 nm
2 nm

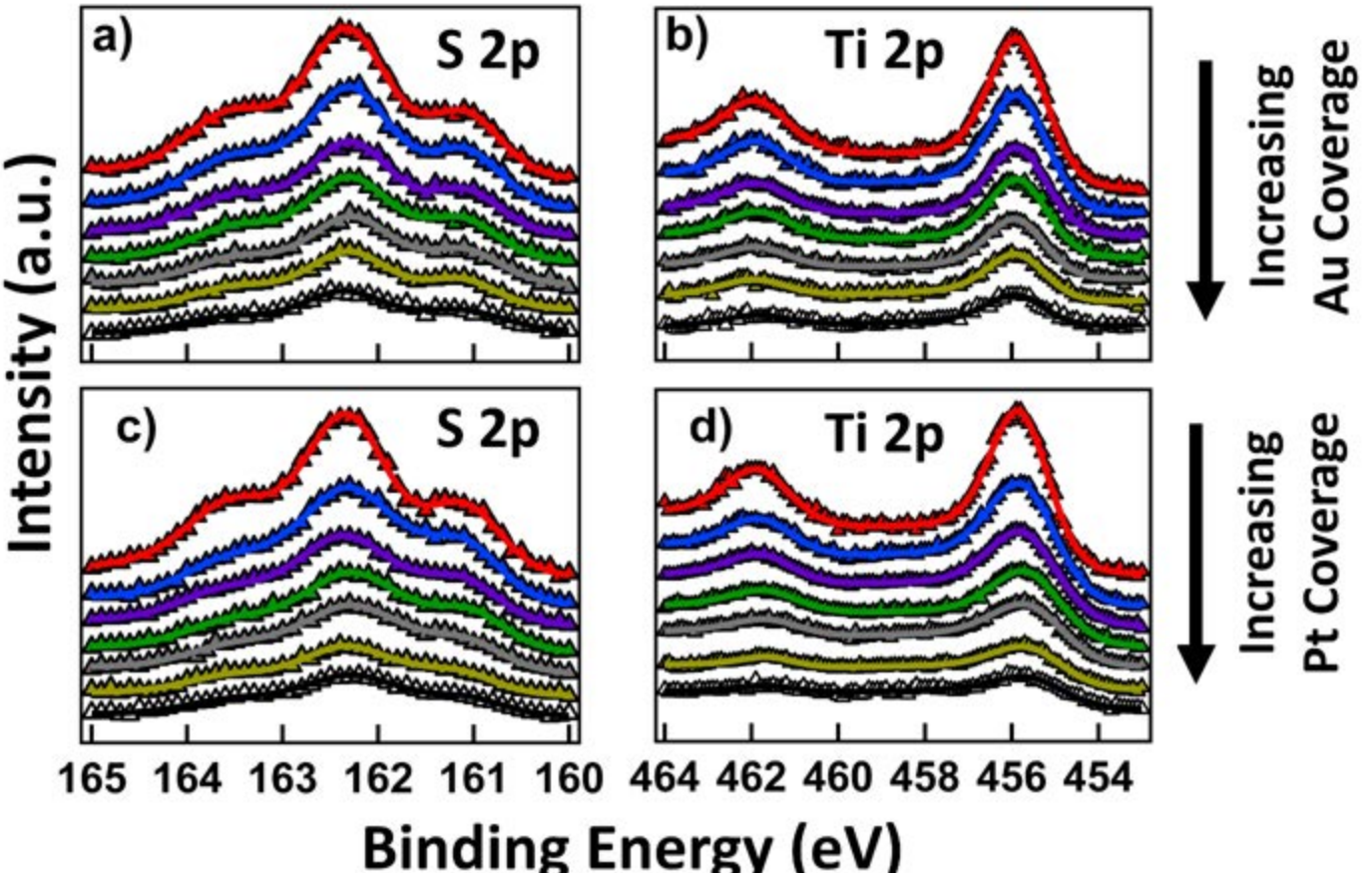
a)
S 2p
b)
Ti 2p
Increasing
Au Coverage
c)
S 2p
d)
Ti 2p
Increasing
Pt Coverage
Intensity (a.u.)
165 164 163 162 161 160
464 462 460 458 456 454
Binding Energy (eV)

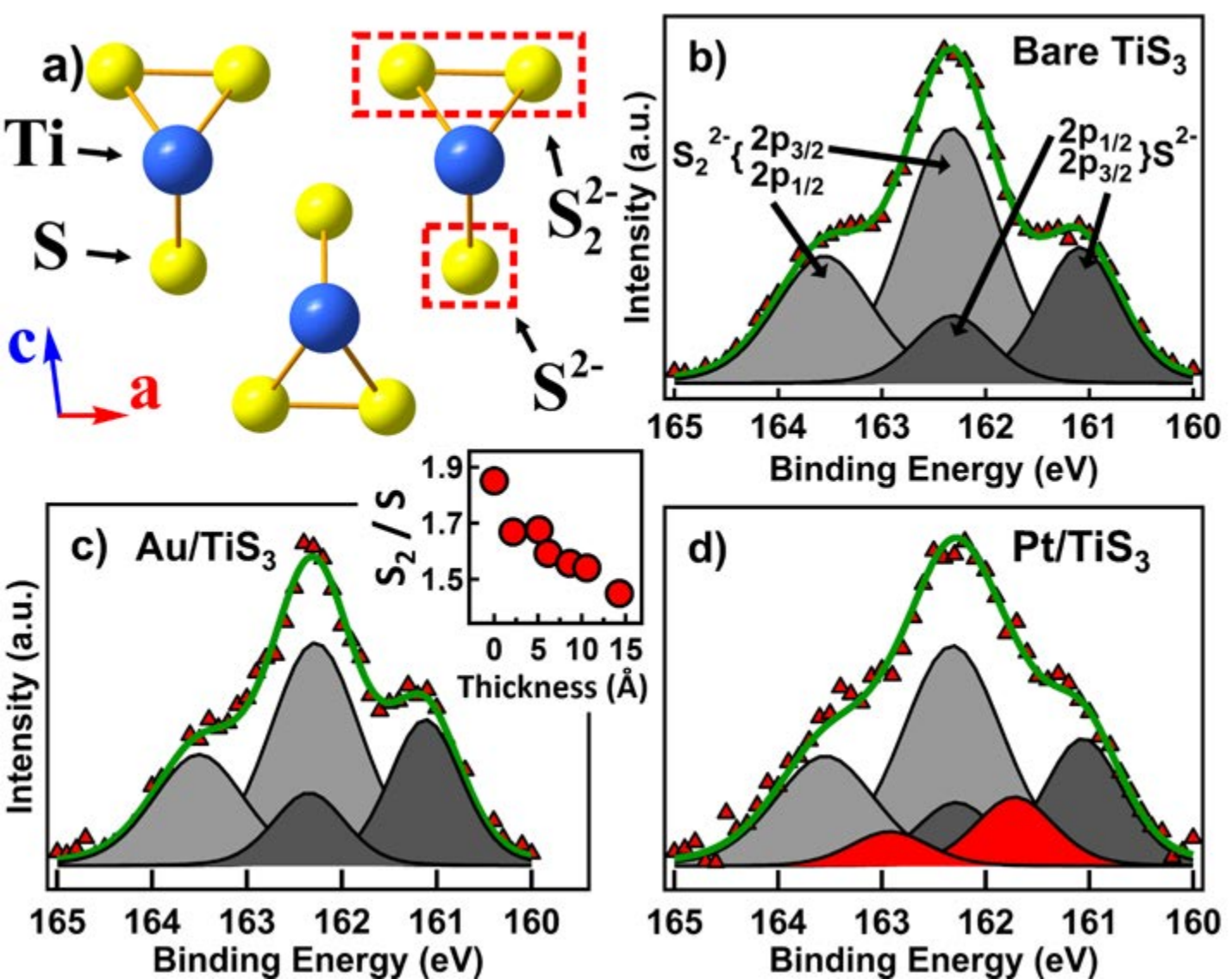
a)
Ti
S
c
a
S_2^{2-}
S^{2-}
b)
Bare TiS_3
Intensity (a.u.)
S_2^{2-} { $2p_{3/2}$ $2p_{1/2}$
$2p_{1/2}$ $2p_{3/2}$ }S^{2-}
165 164 163 162 161 160
Binding Energy (eV)
c) Au/TiS_3
Intensity (a.u.)
S_2 / S
1.9
1.7
1.5
0 5 10 15
Thickness (Å)
165 164 163 162 161 160
Binding Energy (eV)
d)
Pt/TiS_3
165 164 163 162 161 160
Binding Energy (eV)

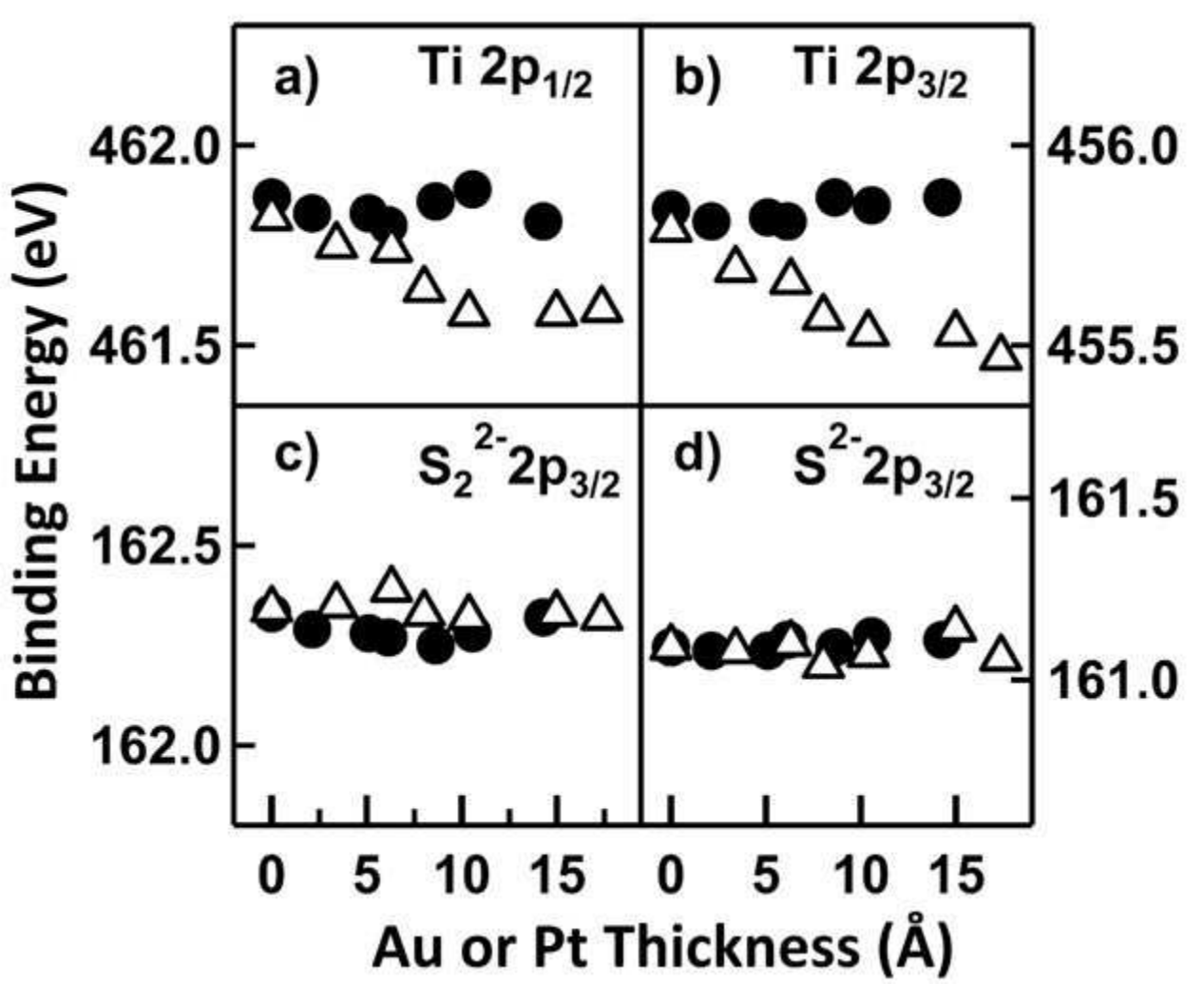
a) Ti 2p1/2
b) Ti 2p3/2
c) S2 2- 2p3/2
d) S 2- 2p3/2
462.0
461.5
456.0
455.5
162.5
162.0
161.5
161.0
0 5 10 15
0 5 10 15
Binding Energy (eV)
Au or Pt Thickness (Å)

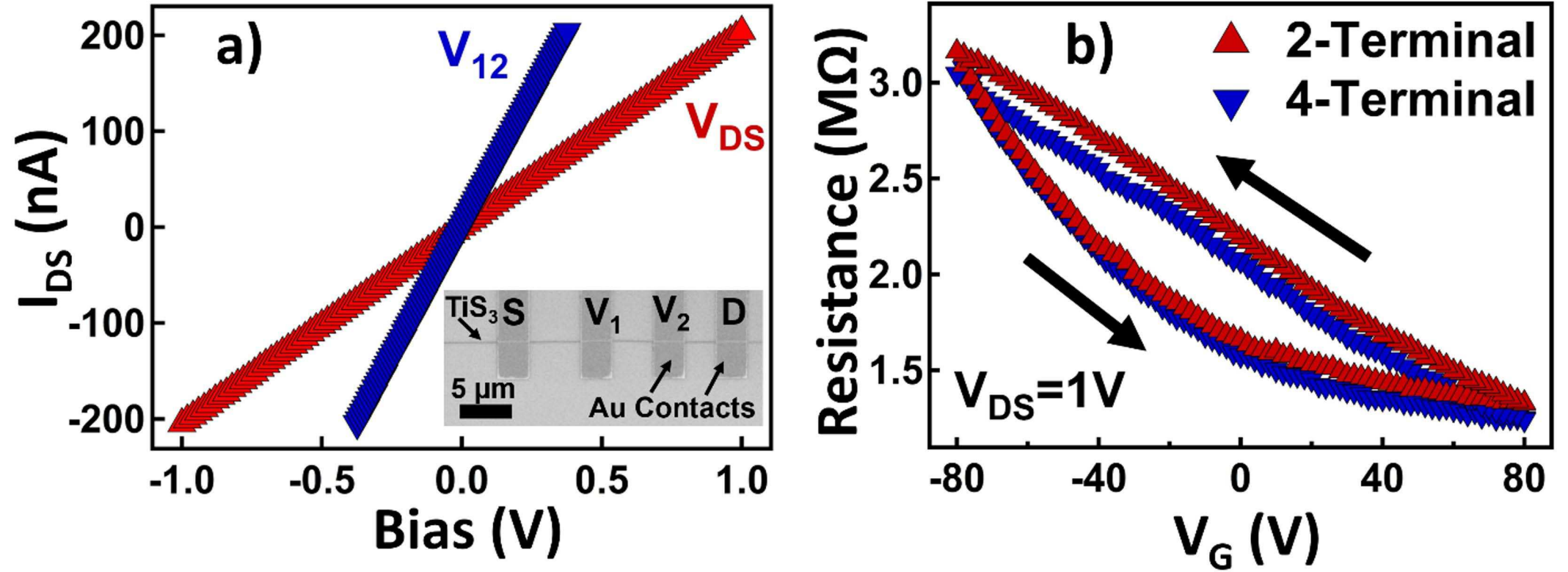
a)
V_{12}
V_{DS}
I_{DS} (nA)
200
100
0
-100
-200
-1.0
-0.5
0.0
0.5
1.0
Bias (V)
TiS_3
S
V_1
V_2
D
5 μm
Au Contacts
b)
2-Terminal
4-Terminal
Resistance (MΩ)
3.0
2.5
2.0
1.5
V_{DS}=1V
-80
-40
0
40
80
V_G (V)